Effects of oxygen vacancy location on the electronic structure and spin density of Co-doped rutile TiO_2 dilute magnetic semiconductors*

Sun Yun-Bin(孙运斌), Zhang Xiang-Qun(张向群), Li Guo-Ke(李国科), and Cheng Zhao-Hua(成昭华)†

State Key Laboratory of Magnetism, Beijing National Laboratory for Condensed Matter Physics, Institute of Physics, Chinese Academy of Sciences, Beijing 100190, *China*

(Received 4 October 2011; revised manuscript received 3 November 2011)

According to density functional theory (DFT) using the plane wave base and pseudo-potential, we investigate the effects of the specific location of oxygen vacancy (V_O) in a (Ti,Co)O_6 distorted octahedron on the spin density and magnetic properties of Co-doped rutile TiO_2 dilute magnetic semiconductors. Our calculations suggest that the V_O location has a significant influence on the magnetic moment of individual Co cations. In the case where two Co atoms are separated far away from each other, when the V_O is located at the equatorial site of a Co-contained octahedron, the ground state of the two Co cations is $d^6(t_{2g}^3\uparrow, t_{2g}^3\downarrow)$ without any magnetic moment. However, if the V_O is located at the apical site, these two Co sites have different ground states and magnetic moments. The spin densities are also observed to be modified by the exchange coupling between the Co cations and the location of V_O. Some positive spin polarization is induced around the adjacent O ions.

Keywords: oxygen vacancy, impurity distribution, electronic structure

PACS: 75.50.Pp, 61.72.jd, 75.30.Hx, 75.10.Lp **DOI:** 10.1088/1674-1056/21/4/047503

1. Introduction

Recently, a lot of work has been done to explore dilute magnetic semiconductors (DMSs) with Curie temperature (T_C) above room temperature because of their potential applications in spintronics.[1−3] Since Matsumoto *et al.*[4] reported that Co-doped anatase TiO_2 films can keep ferromagnetic order up to 400 K, the structures and the magnetic properties of transition metals (TM=Fe, Co, Mn or other metals), doped TiO_2 DMS films and single crystals have been investigated experimentally[5−10] and theoretically.[11−15] Both experimental results and first-principles electronic structure calculations suggest that the TM impurities and O vacancies play important roles in determining the magnetic properties. Using the first-principles density-functional approaches, Yang *et al.*[12] suggested that Co atoms prefer non-uniform distribution with short Co–Co distance, and the short Co–Co distance is crucial for the stability of ferromagnetic coupling. Based on the density functional calculations of Fe-doped TiO_2 with and without V_O, Chen *et al.*[13] found that the oxygen vacancies enhanced the ferromagnetic coupling between Fe dopants. Previous studies indicated that the magnetic properties of Co-doped TiO_2 are strongly dependent on oxygen deficiencies and are sensitive to the form of the sample as well as the preparation methods.[16−19] For example, recent measurements yield a spontaneous magnetization value of 1.1 μ_B/Co for the films which were highly insulated from Co cations in the +2 state,[20] whereas a value of 0.32 μ_B/Co was reported by Matsumoto *et al.*[4] The controversial results suggest that the magnetic properties are significantly modified by the distributions of Co impurities and V_O in TiO_2. Since it is very difficult to obtain information about reduced Co–TiO_2 purely by experimental means since the location of V_O cannot be strictly controlled, knowledge and understanding of the specific defect types and their contributions to magnetic properties will be key to interpreting the experimental data correctly. Although first-principles calculations were performed to investigate the influence of vacancy position on the magnetic properties of Co-doped TiO_2,[21,22] the effect of V_O location at the specific site of the (Ti,Co)O_6 octahedron on the local crystal electric field, in particular on the spin states of the Co-doped TiO_2, are not yet well

*Project supported by the National Basic Research Program of China (Grant Nos. 2009CB929201, 2010CB934202, and 2011CB921801) and the National Natural Sciences Foundation of China (Grant Nos. 50931006, 50721001, and 11034004).

†Corresponding author. E-mail: zhcheng@iphy.ac.cn

© 2012 Chinese Physical Society and IOP Publishing Ltd

understood. In this work, we calculate the electronic structures, the spin densities and the magnetic properties of Co-doped rutile TiO_2 DMS with various configurations. It is found that the electronic state, the spin density distribution, and the magnetic property can be modified by the location of V_O.

2. Method of calculation

The calculations were carried out using the Vienna *ab initio* Simulation Package (VASP).[23] We used the projector augmented-wave (PAW) pseudopotential and the local spin-density approximation (LSDA) to describe the electron–ion interaction and the exchange interaction.[24] The high-energy cutoff for plane wave was set to be 500 eV. Rutile TiO_2 is a tetragonal structure with a space group of $P4_2/mnm$. Two Ti^{4+} cations are located at (0, 0, 0) and (1/2, 1/2, 1/2) and four O^{2-} anions are located at (1±u, 1±u, 0) and (1/2±u, 1/2±u, 1/2) in the unit cell, respectively. In this calculation we used a supercell of $2 \times 2 \times 4$ containing 96 atoms and $3 \times 3 \times 3$ gamma-center k points. Both the supercells of undoped and doped TiO_2 were relaxed using the conjugate-gradient algorithm (CGA) until the Hellman–Feynman force was lower than 0.01 eV/Å (1 Å=0.1 nm). The electronic state relaxation was taken until the energy difference between two self-consistent circulations was lower than 10^{-6} eV. Using the same condition, the calculation in the generalized gradient approximation (GGA) was done for the Co-doped TiO_2 system. Since previous work suggested that the LSDA and GGA calculations gave similar results for this system,[25] we perform only the LSDA calculations.

3. Results and discussion

The structure of undoped rutile in our calculation was optimized into a tetragonal with $a = 4.59$ Å, $c = 2.92$ Å, and $u = 0.304$, which is comparable to the experimental data at 15 K[26] and previously calculated results on the basis of the full-potential linearized augmented plane-wave (FP-LAPW) method.[14] Each Ti^{4+} ion is located in the centre of a distorted octahedron formed by six O^{2-} ions, with the length of the two apical Ti–O_{ap} bonds slightly longer than the four equatorial Ti–O_{eq} bonds. The calculated apical and equatorial bond lengths are 1.973 Å and 1.938 Å, respectively. The four equatorial oxygen atoms form a rectangle, stretched along the c axis, and the apical direction of the octahedron is along the [110] direction. Both the apical and equatorial Ti–O bond lengths decrease slightly with the substitution of Co for Ti and the introduction of V_O into the cell (Table 1).

Table 1. The calculated energies, Co–O bond lengths, and magnetic moments for various configurations of Co-doped rutile TiO_2 with and without oxygen vacancy (V_O). FM stands for ferromagnetic, AFM for antiferromagnetic, and PM for paramagnetic.

Unit cells	Configurations	E/eV	d^{eq}/Å	d^{ap}/Å	$M_{Co}{}^{a}/\mu_B$	$M_{Co}{}^{b/c/d}/\mu_B$	$M_O{}^{eq}/\mu_B$	$M_O{}^{ap}/\mu_B$	M_{Total}/μ_B
$Ti_{32}O_{64}$		−929.144	1.938	1.973			0.00	0.00	0.00
$CoTi_{31}O_{64}$	Co^a	−921.679 (FM)	1.871	1.892	0.61		0.03	0.03	0.92
		−921.644 (PM)							
$Co_2Ti_{30}O_{64}$	Co^a,Co^b	−914.662 (FM)	1.809	1.901	0.61	0.61	0.22	0.00	1.96
		−914.555 (AFM)							
		−914.556 (PM)							
	Co^a,Co^c	−914.286 (FM)	1.833	1.893	0.54	0.54	0.20	0.01	1.60
		−914.242 (AFM)							
		−914.229 (PM)							
	Co^a,Co^d	−914.166 (FM)	1.872	1.897	0.64	0.64	0.04	0.01	1.93
		−914.156 (AFM)							
		−914.088 (PM)							
$Ti_{32}O_{63}$	V_O	−919.171	1.896	1.955			0.00	0.00	0.00
$CoTi_{31}O_{63}$	Co^a,V_O^0	−913.564 (FM)	1.901	1.922	0.86		0.07	0.00	1.07
		−913.440 (PM)							
	Co^a,V_O^1	−913.496 (FM)	1.882	1.893	0.86		0.01	0.04	1.04
		−913.380 (PM)							
	Co^a,V_O^2	−913.577 (FM)	1.865	1.944	0.30		0.00	0.01	0.52
		−913.574 (PM)							

Table 1. (Continued)

Unit cells	Configurations	E/eV	$d^{\rm eq}$/Å	$d^{\rm ap}$/Å	$M_{\rm Co}{}^{a}/\mu_{\rm B}$	$M_{\rm Co}{}^{b/c/d}/\mu_{\rm B}$	$M_{\rm O}{}^{\rm eq}/\mu_{\rm B}$	$M_{\rm O}{}^{\rm ap}/\mu_{\rm B}$	$M_{\rm Total}/\mu_{\rm B}$
$Co_2Ti_{30}O_{63}$	Co^a,Co^b,V_O^0	−906.675 (FM)	1.799	1.880	0.76	0.76	0.13	0.01	2.13
		−906.630 (AFM)							
		−906.169 (PM)							
	Co^a,Co^b,V_O^1	−906.773 (FM)	1.834	1.883	1.33	0.12	0.08	0.07	1.99
		−906.611 (PM)							
	Co^a,Co^d,V_O^0	−906.722	1.853	1.873	0.00	0.00	0.00	0.00	0.00
	Co^a,Co^d,V_O^1	−906.701 (FM)	1.869	1.877	1.44	0.02	0.04	0.09	1.97
		−906.495 (PM)							

We consider the cases where Ti atoms are substituted by one and two Co atoms in the $2 \times 2 \times 4$ supercell (32 Ti or Co and 64 O atoms) of the rutile structure corresponding to a concentration of $x = 1/32$, and $1/16$ and V_O is introduced into the $(Co_xTi_{1-x})O_{2-\delta}$ by removing O anions. The specific sites of Co and V_O located in the supercell are marked in Fig. 1 as letters (a, b, c, or d) and numbers (0, 1, or 2), respectively. The calculated energies of various configurations are summarized in Table 1. The calculated substitution energy of Co, defined as $E^{\rm S}({\rm Co}) = E({\rm CoTi_{31}O_{64}}) + E^{\rm b}({\rm Ti}) - E^{\rm b}({\rm Co}) - E({\rm Ti_{32}O_{64}})$ for one single Co substitution ($E^{\rm b}({\rm Ti}) = -8.472$ eV, and $E^{\rm b}({\rm Co}) = -7.814$ eV, are the energies of bulk hcp Ti and Co, respectively) is 7.671 eV/atom. The large substitution energy implies that the Co doping TiO_2 is less energetically favourable. The substitution energies of two Co atoms in the supercell are comparable to those of one single Co substitution. As for two substitutional Co in $Co_2Ti_{30}O_{64}$ supercells, we compare the energies of two Co cations located at the a, b sites, a, c, and a, d sites, namely the (Co^a,Co^b), (Co^a,Co^c), and (Co^a,Co^d) configurations, respectively. The corresponding distances between the two Co impurities are 2.78 Å, 3.34 Å, and 5.84 Å. The total energy of the (Co^a,Co^b) configuration is the lowest among the three configurations, and is about 0.5 eV lower than that of the (Co^a,Co^d) configuration. Therefore, one can conclude that Co impurities prefer the doping mode with shorter Co–Co distance without V_O.

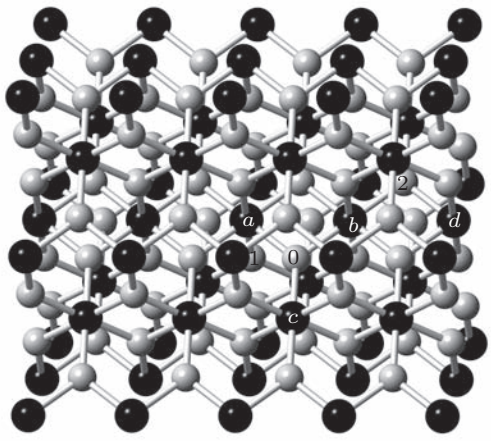


Fig. 1. Configurations of Co and V_O in the 2×2×4 supercell of rutile TiO_2. The black and gray balls represent Ti(Co) and O(V_O), respectively. The specific sites of Co and V_O are marked as letters (a, b, c, or d) and numbers (0, 1, or 2), respectively.

The introduction of one single V_O also results in a large substitution energy. $E^S(V_O) = E({\rm Ti_{31}O_{63}}) + E^{\rm b}({\rm O}) - E({\rm Ti_{32}O_{64}}) = 4.735$ eV ($E^{\rm b}({\rm O}) = -5.238$ eV is the total energy of an O atom in an O_2 molecule. In the case of one Co cation and one V_O in the $Co_1Ti_{31}O_{63}$ supercell, there are two possibilities of removing an oxygen atom: (i) from the Co-contained octahedron (Co^a, $V_O{}^0$) or (Co^a, $V_O{}^1$), and (ii) from the Ti-contained octahedron (Co^a, $V_O{}^2$). Consistent with the results reported by Park *et al.*,[21] our total energy calculations suggest that the V_O near the Ti site is more stable than near Co site. The fact that the V_O prefers to be apart from the Co is also evident when comparing the energy of V_O located at the equatorial site with that at the apical site of the octahedron, namely the (Co^a, $V_O{}^0$) and (Co^a, $V_O{}^1$) configurations in the $CoTi_{31}O_{63}$ supercell, respectively, where the former configuration has a longer Co–O bond length. It can be found that the total energy of the (Co^a, $V_O{}^0$) configuration is slightly lower than that of the (Co^a, $V_O{}^1$) configuration. The Co doping mode is quite different in the presence of V_O. The energy difference decreases to 0.05 eV, suggesting that the preferable distribution of Co in the shorter distance is not remarkable. Both the energetically highest and lowest configurations have short Co–Co distances in the four configurations which contain two Co cations and one V_O. The configuration with the short Co–Co distance is energetically higher than that with the larger Co–Co distance when one of its equatorial O anions is removed, and energetically lower than the later configuration when one of its apical O anions is removed,

which shows a complex dependence of the distribution of Co cations on the location of V_O.

The density of states (DOS) demonstrates that pure TiO_2 shows a semiconducting state. The conduction band and the valence one are contributed mainly by the Ti^{4+} state and the O^{2-} state, respectively. The Fermi level (E_f) is located at the centre of the band gap (Fig. 2(a)). As shown in Fig. 2(b), the DOS of $CoTi_{31}O_{64}$ demonstrates that the Ti and O states are not affected very much by Co doping, and that the Fermi level passes through the valence band. The d-orbitals of Co split into a triply-degenerate t_{2g} state with lower energy and a doubly-degenerate e_g state with higher energy if a cation is placed in an octahedral crystal electric field. Since the lengths of two apical Co–O bonds are slightly longer than those of the other four equatorial Co–O bonds, the e_g state will further split into an energetically lower d_{z^2} state and an energetically higher $d_{x^2-y^2}$ one. The t_{2g} and the e_g states of Co are located near the valence band maximum (VBM) and the conduction band minimum (CBM), respectively. As in the antase Co:TiO_2,[21] one single Co doping results in the half-metallic nature in the system. The occupied electronic configuration of Co is $d^5(t_{2g}^3\uparrow, t_{2g}^2\downarrow)$. The calculated total magnetic moments in the supercell of $CoTi_{31}O_{64}$ and in the atomic sphere of Co with a radius of 1.302 Å are 0.92 μ_B and 0.61 μ_B, respectively.

In the case of two substitutional Co cations in the $Co_2Ti_{30}O_{64}$ supercell, we compare the DOSs for three possible arrangements of Co atoms, (Co^a,Co^b), (Co^a,Co^c), and (Co^a,Co^d). The DOS of the (Co^a,Co^b) configuration shows that the t_{2g} and e_g states of Co cations located near the VBM and CBM become more broad due to the overlap of partial DOS from these two Co sites (Fig. 2(c)). As shown in Fig. 2(d), the individual contribution of two Co sites to DOS is more noticeable when the Co–Co separation is about 3.34 Å, (Co^a,Co^c) configuration. If the Co–Co separation is far away, the DOS of the (Co^a,Co^d) configuration (Fig. 2(e)) is almost the same as the DOS of $CoTi_{31}O_{64}$ (Fig. 2(b)). The magnetic moments of Co atoms at different sites are summarized in Table 1. Th PM state is energetically higher than the FM state for all of the calculated structures, and also higher than the AFM state expect the (Co^a,Co^b) configuration, of which the AFM state and the PM state have similar energy. It is noteworthy that the exchange interaction between Co atoms is strongly dependent on the spatial separation. In the (Co^a,Co^b) configuration, the distance between the two Co impurities was 2.78 Å along the c axis. Exchange parameter J is defined as the energy difference between AFM and FM states, and the same definition has been used by Chen and his co-workers.[13] J was calculated to be 107 meV, which is almost the same as that in the bulk fcc Ni (108 meV with two Ni atoms in the unit cell). With the Co–Co distance increasing up to 5.84 Å, i.e. the (Co^a,Co^d) configuration, the exchange parameter J decreases to about 10 meV. Obviously, the shorter Co–Co distance is required to stabilize the ferromagnetic ordering. Owing to the various possible Co distributions in TiO_2, it is expected that the Curie temperature of Co–TiO_2 DMS could be higher than room temperature.

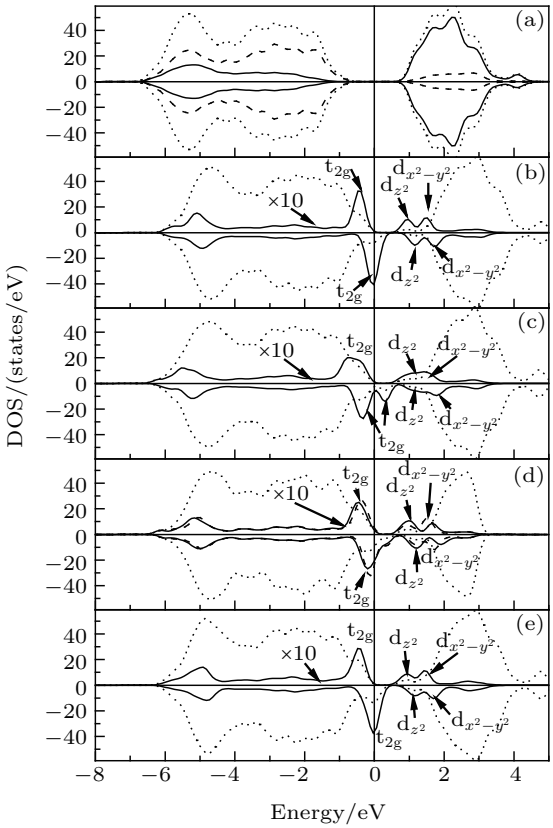


Fig. 2. Calculated total (dot) and partial DOS for Ti (solid), Co (solid or dash), and O (dash) in undoped and various cases of Co-doped TiO_2 rutile: (a) undoped $Ti_{32}O_{64}$, (b) (Co^a) configuration in the $CoTi_{31}O_{64}$ cell, (c) (Co^a,Co^b) configuration, (d) (Co^a,Co^c) configuration, and (e) (Co^a,Co^d) configuration in $Co_2Ti_{32}O_{64}$. The Fermi energy is set to be zero, the positive DOS values are for the spin majority channel, and the negative values are for spin minority channel.

The exchange coupling between two Co atoms is also visible from the spin density. Figure 3 illustrates the spin densities of three cases of Co atoms in the supercell (Co^a), (Co^a,Co^b), and (Co^a,Co^c) configurations. The spin densities indicate that the magnetic

moment arises mainly from the d_{zx} and d_{yz} states of the Co impurities and the p_z state of their nearest neighbouring O anions. The transfer of electrons between the spin minority p state of the equatorial O^{2-} anions and the t_{2g} spin minority state of Co impurity leads the O^{2-} to have a small magnetic moment (Fig. 3(a)). For the (Co^a,Co^b) configuration, some positive spin polarizations are induced around the adjacent O ions due to the strong exchange coupling between two Co ions (Fig. 3(b)). The contribution of the O ion magnetic moment is about 0.22 μ_B. With the Co–Co distance increasing, i.e. the (Co^a,Co^c) configuration, the weak exchange coupling between two Co ions results in the O magnetic moment reducing to about 0.20 μ_B (Fig. 3(c)). If the Co–Co separation is far away, i.e. the (Co^a,Co^d) configuration, the spin densities (not shown) are almost the same as those in Fig. 3(a).

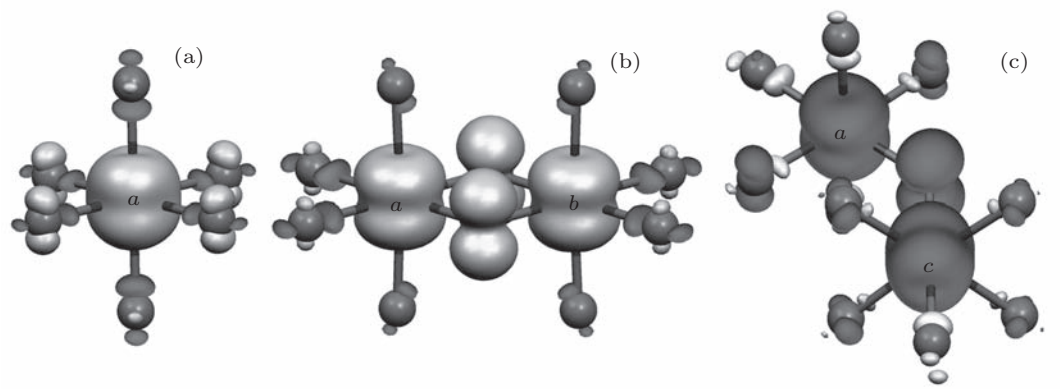


Fig. 3. Spin densities of various cases of Co-doped TiO_2 rutile: (a) (Co^a) configuration, (b) (Co^a,Co^b) configuration, and (c) (Co^a,Co^c) configuration. The isosurface of majority spin density (light gray) has a correlated spin density of 0.05 $\mu_B/Å^3$. The isosurface of minority spin density (dark gray) has a correlated spin density of -0.01 $\mu_B/Å^3$. The dark gray balls represent O anions, and the Co cations are surrounded by the isosurface.

One single V_O in $Ti_{32}O_{64}$ introduces two additional electrons in the conduction band. The DOS pattern of the V_O system, as shown in Fig. 4(a), demonstrates that the electrons are populated at the bottom of the conduction band consisting of the Ti-3d orbitals and delocalized over the entire crystal. However, the DOS remains spin unpolarized. Therefore, based on our calculation, the V_O does not induce a magnetic moment without cation vacancy or TM dopants and the total magnetic moment of the system is zero. Although Hong *et al.*[27] stated that the ferromagnetism in the undoped TiO_2 samples originates from V_O,[27] more and more, theoretical studies support the conclusions that the cation vacancy can induce the magnetic moment, whereas V_O cannot.[28–30]

Experimentally, the accurate determination of the location and the concentration of V_O in Co-doped TiO_2 is very difficult. Computational calculations provide the possibility for understanding the relationship between the V_O location and the magnetic properties. In the case of one Co and one V_O in the $Co_1Ti_{31}O_{63}$ supercell, the valence of Co becomes Co^{2+} in the ionic picture. For the V_O near the Co site, the electronic structure of Co is drastically changed. By removing an O from the CoO_6 octahedron, the weakened crystal field decreases the band gap between the t_{2g} and e_g states, and more electrons that are filled into Co impurity enhance the Fermi level. Therefore, the $3d^7$ electronic state of Co^{2+} contains a full-filled t_{2g} state and a partial filled spin majority e_g state, and consequently Co^{2+} forms in the $d^7(t_{2g}^3 \uparrow e_g^1 \uparrow, t_{2g}^3 \downarrow)$ state. For the (Co^a,V_O) configuration, where V_O is located at one equatorial site of the Co-contained octahedron, the absence of one equatorial O^{2-} makes the crystal electric field weaker in the basal plane. The $d_{x^2-y^2}$ state of Co will have lower energy than the d_{z^2} state (Fig. 4(b)). For the ($Co^aV_O{}^1$) configuration, where V_O is located at one apical site of the Co-contained octahedron, the crystal electric field in the apical direction of the octahedron will be weakened. The lowest unfilled state of Co impurity is the spin minority d_{z^2} state, which is located at the top of the valence band (Fig. 4(c)). On the other hand, if the V_O is far away from the Co site, i.e. the (Co^a, $V_O{}^2$) configuration, then the Fermi level cuts the spin majority d_{z^2} state of Co (Fig. 4(d)). The magnetic moment of Co is slightly enhanced by the nearest neighbouring

V_O (Table 1).

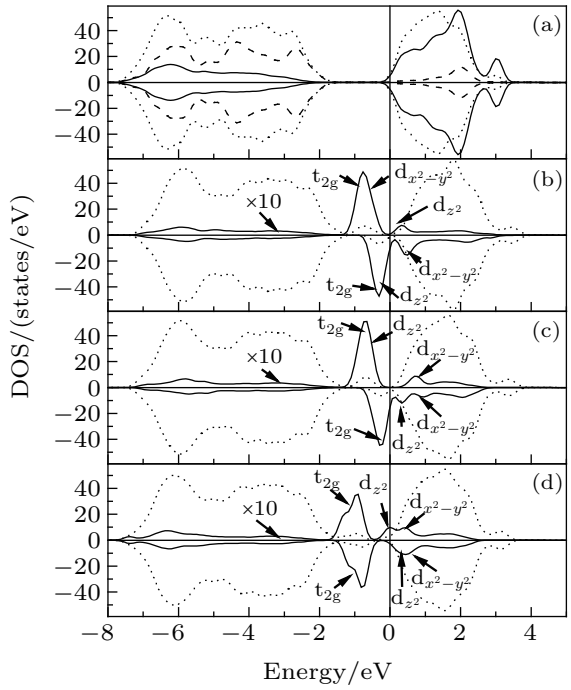


Fig. 4. Calculated total (dot) and partial DOSs for Ti (solid), Co (solid), and O (dash) in various cases of one single Co cation; doped in TiO_2 rutile with one V_O. (a) $Ti_{32}O_{63}$, (b) (Co^a,$V_O{}^0$) configuration, (c) (Co^a,$V_O{}^1$) configuration, and (d) (Co^a,$V_O{}^2$) configuration in $CoTi_{31}O_{63}$. The Fermi energy is set to be zero, the positive DOS values are for the spin majority channel, and the negative values are for the spin minority channel.

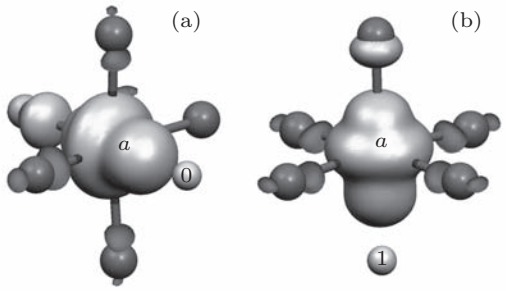


Fig. 5. Spin densities of various cases of one single Co doped in TiO_2 rutile with one V_O: (a) (Co^a,$V_O{}^0$) configuration and (b) (Co^a,$V_O{}^1$) configuration in $CoTi_{31}O_{63}$. The isosurface of majority spin density (light gray) has a correlated spin density of 0.05 $\mu_B/Å^3$. The isosurface of minority spin density (dark gray) has a correlated spin density of -0.01 $\mu_B/Å^3$. The dark gray balls represent O anions and the light gray balls marked with 0 or 1 represent the location of V_O.

The effect of V_O location on the spin density is also evident. Figure 5 illustrates the spin densities of the two cases of one Co and one V_O in the supercell ($Co^a, V_O{}^0$) and ($Co^a, V_O{}^1$) configurations. For the ($Co^a, V_O{}^0$) configuration, the spin density indicates that the magnetic moment arises mainly from the $d_{x^2-y^2}$ state. The spin of the O located at the diagonal site of the V_O site in the basal plane is polarized with a small magnetic moment of 0.07 μ_B (Fig. 5(a)). On the other hand, for the ($Co^a, V_O{}^1$) configuration, the spin density indicates that the magnetic moment arises mainly from the d_{z^2} state, and the spin of the other O located at the apical site is polarized with a small magnetic moment of 0.04 μ_B (Fig. 5(b)). Furthermore, some Ti ions near V_O are observed to possess a small amount of magnetic moment (0.02 μ_B–0.04 μ_B).

Now we consider the case of two Co cations and one V_O in the $Co_2Ti_{30}O_{63}V_O$ supercell. For the arrangement of (Co^a,Co^b,$V_O{}^0$), the DOS shows that the t_{2g} and the e_g states of the Co cation are broader due to the overlap of partial DOS from the Co^a and Co sites (Fig. 6(a)). Both Co^a and Co^b are located in the same crystal electric field. Therefore, the magnetic moments of the Co cation at these two sites have the same values (0.76 μ_B). The total energy calculation demonstrates that the ground state for the (Co^a,Co^b,$V_O{}^0$) configuration in the $Co_2Ti_{30}O_{63}V_O$ supercell is FM and the total magnetic moment is 2.13 μ_B. The local crystal electric fields of two Co atoms are different for the (Co^a,Co^b,$V_O{}^1$) configuration, and the individual contribution of two Co sites to DOS is clearly observed from Fig. 6(b). If the two Co atoms are separated far away, up to 5.84 Å along the c axis, i.e. the (Co^a,Co^d) configuration, then the V_O location has a significant influence on the electronic structure and hence the magnetic moment of individual Co. When V_O is located at the equatorial site of a Co-contained octahedron, the (Co^a,Co^d,$V_O{}^0$) configuration, the electrostatic field energy will be higher than the exchange split energy. Thus, the t_{2g} spin minority states will energetically be lower than the $d_{x^2-y^2}$ spin majority state (Fig. 6(c)). The ground state will be d^6 ($t_{2g}^3\uparrow, t_{2g}^3\downarrow$), and the numbers of filled electrons are the same in the spin majority and spin minority states, which do not induce any magnetic moment of Co. However, if a V_O is located at the apical site of the Co-contained octahedron, the (Co^a,Co^d,$V_O{}^1$) configuration, then the partial DOS patterns (Fig. 6(d)) show that the Co^a and Co^d sites have different ground states, ($t_{2g}^3\uparrow e_g^\alpha\uparrow, t_{2g}^{3-\alpha}\downarrow$) and ($t_{2g}^3\uparrow, t_{2g}^3\downarrow$), corresponding to magnetic moments of 1.44 μ_B and 0.02 μ_B, respectively. The total magnetic

moment for the (Co^a,Co^d,$V_O{}^1$) configuration in the $Co_2Ti_{30}O_{63}V_O$ supercell is 1.97 μ_B.

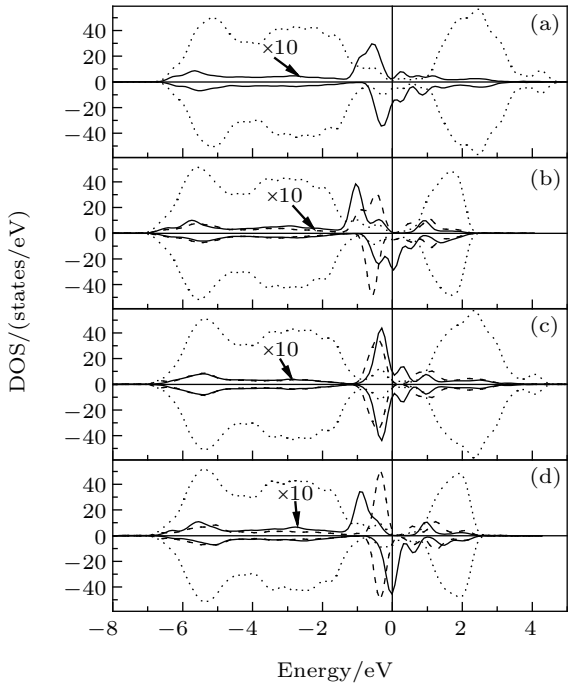


Fig. 6. Calculated total (dot) and partial DOSs for Co (solid or dash) in various cases of 2Co and $1V_O$ in the supercell of $Co_2Ti_{30}O_{63}$: (a) (Co^a, Co^b,$V_O{}^0$), (b) (Co^a, Co^b,$V_O{}^1$), (c) (Co^a, Co^d,$V_O{}^0$), and (d) (Co^a, Co^d,$V_O{}^1$) configurations. The Fermi energy is set to be zero, the positive DOS values are for the spin majority channel, and the negative values are for the spin minority channel.

Figure 7 illustrates the spin densities of three cases of two Co cations and one V_O in the supercell, (Co^a,Co^b,$V_O{}^0$), (Co^a,Co^b,$V_O{}^1$), and (Co^a,Co^d,$V_O{}^1$). The spin densities indicate that the magnetic moment is located near the e_g state of Co impurity. For the (Co^a,Co^b,$V_O{}^0$) configuration, the exchange parameter J is 45 meV. The relatively strong exchange coupling between two Co ions results in the spin polarization of the O between two Co atoms in the direction parallel to their magnetic moments (Fig. 7(a). The contribution of the O ion magnetic moment is about 0.12 μ_B. The location of V_O is found to influence the distribution of spin densities (Figs. 6(a) and 6(b)). With a further increase in the Co–Co distance, i.e. the (Co^a,Co^d,$V_O{}^1$) configuration, the weak exchange coupling between two Co cations results in a decrease in O magnetic moment to 0.04 μ_B. From the spin densities of the Co^a and Co^d sites, one can clearly see that spin of Co^a is polarized, whereas the Co^d spin is unpolarized (Fig. 7(c)).

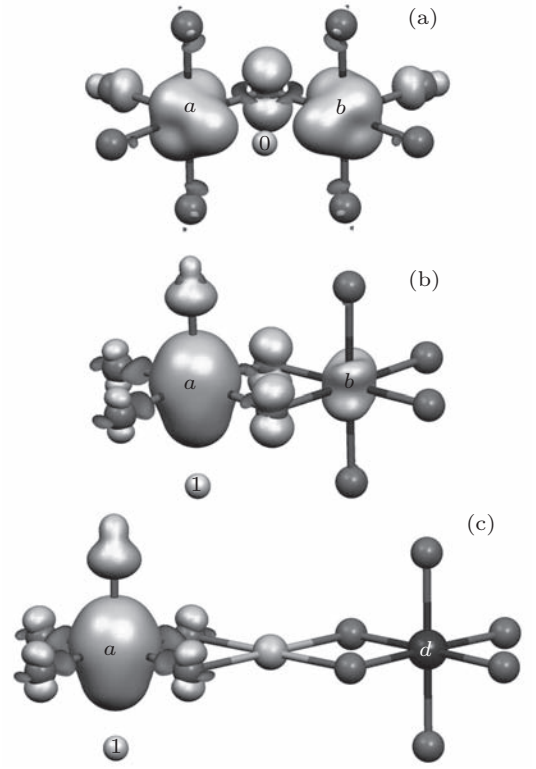


Fig. 7. The spin densities in various cases of 2Co and $1V_O$ in the supercell of $Co_2Ti_{30}O_{63}$: (a) (Co^a, Co^b,$V_O{}^0$), (b) (Co^a, Co^b,$V_O{}^1$), and (c) (Co^a, Co^d,$V_O{}^1$) configurations. The isosurface of majority spin density (light gray) has a correlated spin density of 0.05 $\mu_B/Å^3$. The isosurface of minority spin density (dark gray) has a correlated spin density of -0.01 $\mu_B/Å^3$. The light gray, black, and dark gray balls represent Ti, Co, and O, respectively. The location of V_O is marked with 0 or 1.

4. Conclusions

Our calculations suggest that the specific location of oxygen vacancy in a CoO_6 distorted octahedron strongly influences the distribution, spin density and magnetic properties of Co-doped rutile TiO_2 dilute magnetic semiconductors. Without V_O, Co impurities prefer a doping mode with shorter Co–Co distance, whereas the preferable distribution of Co in shorter distances is not remarkable in the presence of V_O. In the case of two Co atoms that are separated far away from each other, if the V_O is located at the equatorial site of a Co-contained octahedron, then the ground state of two Co cations is d^6 ($t_{2g}^3\uparrow, t_{2g}^3\downarrow$) without any magnetic moment. However, if a V_O is located at the apical site of the Co-contained octahedron, then the two Co sites have different ground states, ($t_{2g}^3\uparrow e_g^\alpha\uparrow, t_{2g}^{3-\alpha}\downarrow$) and ($t_{2g}^3\uparrow, t_{2g}^3\downarrow$), corresponding to magnetic moments of 1.44 μ_B and 0.02 μ_B, respectively. Therefore, our calculation results can explain

the fact that the magnetic properties of Co-doped TiO_2 are strongly dependent on oxygen deficiency and are sensitive to the form of the sample as well as the preparation methods.

References

[1] Ohno H 1998 *Science* **281** 951

[2] Fukumura T, Yamada Y, Toyosaki H, Hasegawa T, Koinuma H and Kawasaki M 2004 *Appl. Surf. Sci.* **223** 62

[3] Coey J M D 2006 *Curr. Opin. Solid State Mater. Sci.* **10** 83

[4] Matsumoto Y, Murakami M, Shono T, Matsumoto Y, Hasegawa T, Fukumura T, Kawasaki M, Ahmet P, Chikyow T, Koshihara S Y and Koinuma1 H 2001 *Science* **291** 854

[5] Hong N H, Sakai J, Prellier W and Hassini A 2003 *Appl. Phys. Lett.* **83** 3129

[6] Shutthanandan V, Thevuthasan S, Heald S M, Droubay T, Engelhard M H, Kaspar T C, McCready D E, Saraf L, Chambers S A, Mun B S, Hamdan N, Nachimuthu P, Taylor B, Sears R P and Sinkovic B 2004 *Appl. Phys. Lett.* **84** 4467

[7] Han G C, Wu Y H, Tay M, Li K B, Guo Z B and Chong T C 2004 *J. Magn. Magn. Mater.* **268** 159

[8] Sangaletti L, Mozzati M C, Galinetto P, Azzoni C B, Speghini A, Bettinelli M and Calestani G 2006 *J. Phys.*: *Condes. Matter* **18** 7643

[9] Hong N H, Sakai J, Ruyter A and BrizéV 2006 *Appl. Phys. Lett.* **89** 252504

[10] Jiang Y B, Mi W B, Jiang E Y and Bai H L 2009 *J. Vac. Sci. Technol.* A **27** 1172

[11] Geng W T and Kim K S 2003 *Phys. Rev.* B **68** 125203

[12] Yang Z X, Liu G and Wu R Q 2003 *Phys. Rev.* B **67** 060402

[13] Chen J, Rulis P, Ouyang L, Satpathy S and Ching W Y 2006 *Phys. Rev.* B **74** 235207

[14] Rubio-Ponce A, Conde-Gallardo A and Olguin D 2008 *Phys. Rev.* B **78** 035107

[15] Peng H W, Li J B, Li S S and Xia J B 2009 *Phys. Rev.* B **79** 092411

[16] Dietl T, Ohno H, Matsujura F, Cibert J and Ferrand D 2000 *Science* **287** 1019

[17] Kim D H, Yang J S, Kim Y S, Kim D W, Noh T W, Bu S D, Park Y D, Pearton S J, Jo Y and Park J G 2003 *Appl. Phys. Lett.* **83** 4574

[18] Manivannan A, Glaspell G, Dutta P and Seehra M S 2005 *J. Appl. Phys.* **97** 10D325

[19] Pan D Y, Xu G L, Lü L Y, Yong Y, Wang X W, Wang J G, Wang G H and Sui Y X 2006 *Appl. Phys. Lett.* **89** 082510

[20] Griffin K A, Pakhomov A B, Wang C M, Heald S M and Krishnan K M 2005 *Phys. Rev. Lett.* **94** 157204

[21] Park M S, Kwon S K and Min B I 2002 *Phys. Rev.* B **65** 161201(R)

[22] Weng H, Yang X, Dong J, Mizuseki H, Kawasaki M and Kawazoe Y 2004 *Phys. Rev.* B **69** 125219

[23] Kresse G and Furthmuller J 1996 *Phys. Rev.* B **54** 11169

[24] Blochl P E 1994 *Phys. Rev.* B **50** 17953

[25] Errico L A, Rentería M and Weissmann M 2005 *Phys. Rev.* B **72** 184425

[26] Burdett J K, Hughbanks T, Miller G J, Richardson J W and Smith J V 1987 *J. Am. Chem. Soc.* **109** 3639

[27] Hong N H, Sakai J, Poirot N and Brize V 2006 *Phys. Rev.* B **73** 132404

[28] Pemmaraju C D and Sanvito S 2005 *Phys. Rev. Lett.* **94** 217205

[29] Bouzerar G and Ziman T 2006 *Phys. Rev. Lett.* **96** 207602

[30] Dev P, Xue Y and Zhang P 2008 *Phys. Rev. Lett.* **100** 117204